Royal Netherlands Institute for Sea Research



Riekenberg, P.M.; Oakes, J.M. & Eyre, B.D. (2020). Shining light on priming in euphotic sediments: nutrient enrichment stimulates export of stored organic matter. *Environmental Science and Technology*, 54, 11165-11172

Published version: https://doi.org/10.1021/acs.est.0c01914

NIOZ Repository: http://imis.nioz.nl/imis.php?module=ref&refid=330292

[Article begins on next page]

# Shining light on priming in euphotic sediments: Nutrient enrichment stimulates export of stored organic matter

Philip M. Riekenberg[1,2*], Joanne M. Oakes[2], Bradley D. Eyre[2]

[1]NIOZ, Royal Netherlands Institute for Sea Research and Utrecht University, Department of Marine Microbiology and Biogeochemistry, PO Box 59, Den Hoorn, 1790AB, Netherlands

[2]Centre for Coastal Biogeochemistry, Southern Cross University, PO Box 157, Lismore, NSW, 2480, Australia

[*] Corresponding author: phrieken@gmail.com +31644994652

Keywords: nutrient enrichment, microphytobenthos, carbon, priming

Teaser: Priming effects drive increased export of organic carbon from refractory sediment organic matter in euphotic intertidal zones.

16 **Author created TOC graphic**

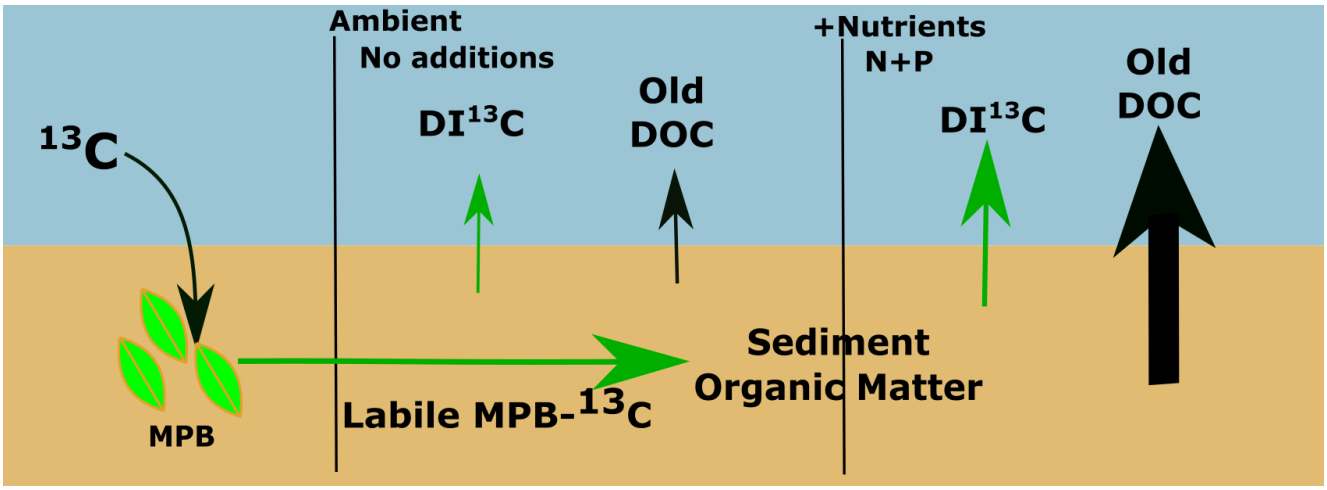


17
18

**Estuarine sediments are important sites for the interception, processing and retention of organic matter, prior to its export to the coastal oceans. Stimulated microbial co-metabolism (priming) potentially increases export of refractory organic matter through increased production of hydrolytic enzymes. By using the microphytobenthos community to directly introduce a pulse of labile carbon into sediment, we traced a priming effect and assessed the decomposition and export of pre-existing organic matter. We show enhanced efflux of pre-existing carbon from intertidal sediments enriched with water column nutrients. Nutrient enrichment increased production of labile microphytobenthos-carbon which stimulated degradation of previously unavailable organic matter and led to increased liberation of "old" (6855 ± 120 years BP) refractory carbon as dissolved organic carbon. These enhanced DOC effluxes occurred at a scale that decreases estimates for global organic carbon burial in coastal systems and should be considered as an impact of eutrophication on estuarine carbon budgets.**

## Introduction

Estuaries, and particularly shallow photic estuarine sediments (<40 m)[1], are hotspots for organic matter (OM) processing, altering terrestrial OM received from rivers prior to its export to the coastal ocean[2-4]. The extent of terrestrial OM processing that occurs along the estuarine continuum largely determines whether estuaries function as carbon (C) sources or sinks[4]. The priming effect describes the additional release of C from a refractory source of OM (pre-existing sediment OM in this study, or added refractory material in others) stimulated by addition of a labile form of C. In terrestrial environments, increased C release from soils is usually measured as evolution of additional $CO_2$ into a headspace from amended treatments (with labile C added) when compared to non-amended controls[5]. Although priming has been well-described and explored within soils[6], priming has only recently gained recognition in aquatic systems. Within aquatic sciences, priming has primarily been investigated as a potential pathway for additional OM processing within settings where heterotrophy dominates (e.g., riverine dissolved OM, hyporheic zone, deep sediment; Fig. 1)[7-10] and has not been consistently demonstrated to occur[11]. Occurrence of priming is highly dependent on substrate composition, sediment structure, and/or microbial community composition[11]. Studies examining priming within coastal benthic zones are limited[8,12,13], but have found positive priming effects within their limited scope (i.e., vial incubations of sediment slurries).

Priming studies in aquatic environments have thus far relied stable or radiocarbon isotope tracers to trace the evolution of $CO_2$ from dissolved inorganic carbon ($DI^{13}C$ or $DI^{14}C$) derived from either labile or refractory C sources (study dependent) to quantify the relative contributions from microbial processing of the $^{13}C$ addition. A number of approaches have been used in various environments in an attempt to identify priming effects, i.e., to demonstrate that microbial

degradation of refractory terrestrial organic C has been stimulated following the addition of labile C[10,14-16]. These approaches use additions of both refractory OM and labile C to stimulate mineralization of added OM[13,17] or pre-existing sediment OM (Fig. 2A)[8,9,12,18]. Addition of unlabeled C (refractory or labile) into the sediment confounds partitioning of export pathways by introducing new OM. Any exported C derived from this newly added OM is indistinguishable from that derived from pre-existing sediment OM. In this study, we used the in situ microphytobenthos (MPB) community to inject a pulse of labile MPB-derived $^{13}C$ (MPB-C) into coastal sediments (Fig. 2B). This approach was intended to preserve both the production (loading rate) and composition (proportion of relative sugars) of priming additions produced daily by diatoms within highly productive shallow coastal environments[12,19]. This method preserves the microbial community, as boundary layers and sediment structure are maintained during label addition with minimal disturbance. This differs from all other priming studies the authors are aware of, which have directly added single labile and/or refractory compounds to homogenized sediment (Fig. 2A)[8,9,12,13,20].

Some priming studies account for both dissolved inorganic C (DIC) and dissolved organic carbon (DOC) pools when identifying additional stimulated breakdown and release of C[8,14-16], but it remains common to solely measure the evolution of DI$^{13}C$ and DIC[9,10,13,18]. This approach works well for systems where heterotrophic evolution of DIC is the only or major pathway for C loss. However, relying on DIC effluxes alone to identify PE becomes problematic in systems where primary production during light exposure uses DIC at rates exceeding the evolution of respired DIC (Fig. 1B). This scenario occurs in shallow coastal benthic sediments, where MPB production causes considerable DIC demand during light periods, which can result in the re-capture and recycling of previously respired carbon. Strong uptake of DIC in euphotic

settings could potentially be wrongly interpreted as a negative priming effect as labeled DIC is recycled and reincorporated into biomass instead of being evolved as $^{13}CO_2$, especially in the case of systems that are DIC-limited or have elevated rates of primary productivity due to eutrophication. We argue that recycling of DIC in euphotic sediments can be partially offset by refining the definition of priming to encompass all C exported during remineralizationof refractory OM (i.e., including DOC effluxes from sediment OM). Measuring priming effects using the evolution of DOC in addition to DIC from both labile and refractory OM sources will account for all substrates produced by the microbial community during remineralization.

Priming has a large effect on organic C processing in soils, as labile C additions stimulate the breakdown of more recalcitrant OM, often doubling rates of remineralization[21]. Priming appears to occur across all terrestrial ecosystems that have been examined and impacts global terrestrial C budgets[22]. Priming has not been clearly shown to impact photic aquatic systems and remains an unaccounted process in coastal carbon processing that likely affects the form and quantity of exported OM to the coastal oceans. In productive aquatic systems, heterotrophic bacteria are provided with rich algal-derived organic matter that can fuel breakdown of otherwise refractory pre-existing sediment OM as DOC, especially in settings where increased nutrient availability has occurred. Priming in increasingly eutrophic settings is expected to decrease as heterotrophs switch from using refractory sediment OM to using accumulated labile organic matter as it becomes more available[21], but the amount of nutrient enrichment required to trigger decreased priming remains unclear.

In this study, we aimed to use nutrient amendments (N as $NH_4^+$ and phosphorous as $H_3PO_4$) to stimulate processing of labile C from MPB in sediments and induce a priming effect that would release additional stored refractory carbon from coastal sediments. Interactions

between MPB and heterotrophic bacteria were stimulated through an equimolar nutrient addition of N and P equivalent to 2.5× the trigger concentration for increased trophic status under Australian and New Zealand Environment Conservation Council guidelines[21], and through simultaneous monitoring of both DIC and DOC fluxes we were able to detect the priming effect that occurred. We expected priming to cause increased export of DIC from pre-existing C within sediment OM despite high productivity causing DIC uptake (negative DIC fluxes), but additional export of DOC derived from previously stored refractory sediment OM was unexpected.

## Methods

### Site description

In January 2015 a subtropical intertidal shoal was sampled ~2 km upstream of the mouth of the Richmond River estuary in New South Wales, Australia (28°52'30"S, 153°33'26"E) with a semidiurnal tidal range of ~2 m. A number of previous labeling studies have been undertaken at this site[24,25] and this study coincides with another that tracks the short-term processing and fate of MPB-C in the microbial community, sediment, and fluxes[26]. This previous work demonstrated that bacteria have a considerable role in the short-term processing of carbon derived from MPB, but the present study tracks longer-term processing and fate of MPB derived carbon and how microbial processing affected pre-existing sediment OM. Through longer term monitoring of organic matter fluxes, we were able to identify priming within euphotic intertidal sediments for the first time to the authors' knowledge. Site sediment (0-10 cm) was mostly fine sand (66%-73%), with a total organic C content of 17.5±0.02 mol C $m^{-2}$, an average molar C:N ratio of 14.7 ± 1.5, and a MPB assemblage dominated by pennate diatoms. There was no evidence of

cyanobacteria and few heterotrophs (>500 µM) observed under light microscopy (1000 ×). Foraminifera were the dominant heterotrophs (>500 µM) within site sediment.

## Labeling of MPB Exudates

We applied $^{13}C$ as $NaH^{13}CO_3$ to MPB *in situ* to track the production of algal carbon that occurred during a single tidal minimum within the intertidal setting in order to track production and processing of MPB-C. Bare sediment within two experimental plots (1 $m^2$) was labeled with 99% $NaH^{13}CO_3$ (Cambridge Isotope Laboratories, Tewksbury, USA) when sediments were first exposed at low tide, following the method outlined in Oakes and Eyre [24]. Label applications were prepared using NaCl-amended Milli-Q to match site salinity (34.6). Motorised sprayers were used to apply 20 mL aliquots (each containing 1.7 mmol $^{13}C$) to each individual 400 $cm^2$ subplot during a tidal low, resulting in a label application of 42.5 mmol $^{13}C$ $m^{-2}$. This application of individual aliquots of label ensured even $^{13}C$ application across the sediment surface. Over ~4 hours of sediment exposure (average light level of 1376 µE $m^{-2}$ $s^{-1}$), there was incorporation of 1549±140 µmol $^{13}C$ $m^{-2}$ into sediment OC, represented ~1% of the initially added $^{13}C$. The remaining unincorporated $^{13}C$ was flushed from the sediment through tidal inundation of the site immediately following this incorporation (Fig. 2b). This tidal flushing removed 99.0% of the $^{13}C$ from the label application, based on the $^{13}C$ content of sediment OC within the initial cores prior to incubation[26]. Of the $^{13}C$ incorporated into sediment OC, ~46% or 716 µmol $^{13}C$ is expected to be in the form of carbohydrates as calculated from uptake rates for $^{13}C$ presented in Oakes, et al.[19] for mannose, fucose, rhamnose, galactose, glucose, xylose, and OC.

## Incubation setup

Sediment cores (20 cm depth, 9 cm diameter) were taken from the labeled plots during the next low tide after labeling, transported to the laboratory, randomly allocated between treatment tanks, and incubated under two nutrient enrichment scenarios (ambient and elevated) using 2 pulsed nutrient additions. Duplicate cores (n=2) were incubated for each time period (0.5 d, 1.5 d, 2.5 d, 3.5 d and 10.5 d) for each treatment (ambient and elevated, total core n=20). Laboratory core incubations allowed explicit control of nutrient additions, reducing the variability in water quality that occurs naturally across the tidal cycle. Pulsed applications of nutrients were used to mimic a range of nutrient concentrations without exceeding sediment capacity for uptake [26]. Treatment tanks were both initially set up at ambient concentration using site water (unfiltered, salinity 34.6), with N ($NH_4^+$) and P ($H_3PO_4$) amendments added to the elevated treatment tank at 10 × water column concentrations observed previously for this site (4 µmol $L^{-1}$ TN and 5 µmol $L^{-1}$ TP). These nutrient concentrations are comparable to nutrient loading observed in other estuaries subject to eutrophication[27] and are ~2× equimolar concentrations observed in the Richmond River for both TN and TP (25.8 µmol $L^{-1}$ and 24.5 µmol $L^{-1}$, respectively) observed directly after multiple flooding events in the Richmond River [33,28]. The initial pulse of nutrients was added to incubation tanks and bags holding replacement water for sampling shortly prior to cores being randomly allocated to the two incubation tanks. An additional pulse of $NH_4^+$ was applied to the elevated treatment tank at the end of 1.5 d in an effort to mimic the nutrient availability that occurs with regular inundation of tidal sediments, with complete removal of $NH_4^+$ confirmed within 24 h of each application. An addition of sodium metasilicate ($Na_2SiO_3$, added to treatment tanks to achieve 17 µmol Si $L^{-1}$) was added at the end of the 2.5 d to ensure that isolation of the benthic diatom-dominated sediment from regular water turnover did not result in secondary limitation of Si.

168 Benthic flux incubations

169 Cores were fitted with magnetic stir bars positioned 10 cm above the sediment surface and filled
170 with ~2 L of site water. Water in the treatment tanks and cores was continuously recirculated,
171 held at 25 ± 1°C by a chiller on each tank, and aerated via continuous direct injection of ambient
172 air into the water via an air stone. Cores were stirred via a rotating magnet at the center of each
173 treatment tank, which interacted with the magnetic stir bars fitted within each core. Stirring
174 occurred at a rate below the threshold for sediment resuspension[29,30]. Three high pressure sodium
175 lamps (correlated color temperature ~2100)[31] suspended above the treatment tanks provided 824
176 ± 40 μE $m^{-2}$ $s^{-1}$ to the sediment/water interface within the cores on a 12 h light/12 dark cycle.
177 This light level is similar to the measured light level for the in situ site sediment surface during
178 inundation (941.4 ± 139 μE $m^{-2}$ $s^{-1}$).

179 Cores were allowed to acclimate for 6 h before the incubation time began and remained open to
180 the tank water until 30 min before initial sampling when clear Plexiglas lids were fitted to each
181 core liner to seal in overlying water without headspace for the duration of the incubation. Rapid
182 processing of the added MPB-C likely occurred during the 6 h acclimation period, but flux
183 measurements were not possible during re-establishment of sediment redox layers immediately
184 after coring. The acclimation period allowed for a robust baseline to develop prior to sampling
185 for diel water column flux incubations. During sampling, 50 mL of water was syringe-filtered
186 (precombusted GF/F) into precombusted 40 mL glass vials with Teflon coated septa, killed with
187 $HgCl_2$ (20 μL saturated solution), and refrigerated prior to analysis for concentration and $\delta^{13}C$ of
188 DIC and DOC. Initial samples were taken 30 min after closure of the lids, dark samples were
189 taken after ~12 hours incubation with no light, and light samples were taken 3 hours after
190 illumination started at the end of the dark sampling. Measured core duplicates were sacrificed

and sectioned for sediment organic matter measurements at the end of the 3 h light period for each sampling time. Oxygen measurements were taken for the overlying water with oxygen saturation never occurring below 86.1% during the dark incubations (oxygen fluxes presented in Riekenberg, et al. [26]). DIC and DOC concentrations and $\delta^{13}C$ values (‰) were measured via continuous-flow wet oxidation isotope-ratio mass spectrometry using an Aurora 1030W total organic C analyzer coupled to a Thermo Delta V isotope ratio mass spectrometer (IRMS)[32]. Sodium bicarbonate (DIC) and glucose (DOC) of known isotopic composition dissolved in He-purged Milli-Q were used to correct for drift and verify both concentration and $\delta^{13}C$ of samples. Reproducibility was ± 0.2 mg $L^{-1}$ and ± 0.1 ‰ for DIC and ± 0.2 mg $L^{-1}$ and ± 0.4 ‰ for DOC.

Total $^{13}C$ in water column DIC and DOC was calculated for initial, the end of the dark period (12 h), and the end of the light period (3 h) as the product of excess $^{13}C$ (excess $^{13}C$ in labeled sample versus relevant natural abundance control), core volume, and concentration. Total excess flux of $^{13}C$ as DIC or DOC (excess $^{13}C$ $m^{-2}$ $h^{-1}$) was then calculated as:

$$\text{Excess } ^{13}C \text{ flux} = (\text{Excess } ^{13}C_{start} - \text{Excess } ^{13}C_{end}) / SA / t$$

where excess $^{13}C_{start}$ and excess $^{13}C_{end}$ represent excess $^{13}C$ of DIC or DOC at the initial and dark samplings to calculate dark flux and the dark sampling to the end of the light incubation periods to calculate the light flux, SA is sediment surface area, and *t* is incubation period length (h). Net fluxes of excess $^{13}C$ (excess $^{13}C$ $m^{-2}$ $h^{-1}$) for DIC and DOC were calculated as:

Net flux = ((dark flux * dark hours) + (light flux * light hours))/ 24 hours

where dark and light periods were 12/12 representing in situ conditions. Total carbon fluxes for DIC and DOC as well as $DI^{13}C$ and $DO^{13}C$ exported to the water column from initial labeling to each sampling period was interpolated using measured net flux values for each treatment during

each sampling period (0.5 d, 1.5 d, 2.5 d, 3.5 d, and 10.5 d). Carbonate dissolution made a negligible contribution to total $CO_2$ during incubations and therefore no corrections were applied to DIC fluxes[32].

Global flux estimates for DOC (Tg C $yr^{-1}$) were calculated as in Maher and Eyre [33]:

$$DOC_{Glob} = 6.7 * (DOC_{Net} * Inter_{Area} * 365 * 12.011 ) / 10^{15}$$

where 6.7 represents the increased DOC flux observed from priming effects in this study, $DOC_{Net}$ are minimum and maximum average diel DO C fluxes observed in Maher and Eyre[23] (2.7 and 3.7 mmol C $m^{-2}$ $d^{-1}$), $Inter_{Area}$ is the global intertidal area 0.62 ($10^{12}$ $m^2$)[34] , and 12.011 is the atomic mass of carbon required to convert from molar weight to grams of C.

Characterization of DOC Efflux

The UV-visible absorption spectra was measured from 300-700 nm on a Horiba Aqualog using a 1 cm cell. Absorbance (A) is converted to absorption coefficients (a) using $a_{(\lambda)} = 2.303\ A(\lambda) / l$, where $A(\lambda)$ is absorbance at wavelength $\lambda$ and l is the path length of the cell in meters. Spectral slope was determined by fitting $a_{(300\text{-}700)}$ to a single exponential decay function using non-linear regression[35]. The spectral slopes from both 275-295 nm ($S_{275\text{-}290}$) and 350-400 nm ($S_{350\text{-}400}$) were calculated through linear regression of the log transformed spectra. Slopes are reported as positive numbers following mathematical convention. The slope ratio ($S_R$) was calculated as the ratio of $S_{275\text{-}295}$ and $S_{350\text{-}400}$. $S_R$ is inversely related to the molecular size of the chromophoric dissolved organic matter (CDOM) within the sample and is expected to increase with decreasing molecular size.

SUVA 254 (L $mg^{-1}$ $m^{-1}$) is an indicator of relative aromaticity of the molecules comprising the pool of CDOM [36] and is calculated as:

$$SUVA\ 254 = a_{254} / DOC$$

where $a_{254}$ is the absorption coefficient at 254 nm ($m^{-1}$) and DOC is concentration of DOC (mg $L^{-1}$) within the sample. Elevated SUVA 254 indicates the increased presence of aromatic moieties contained within CDOM.

Radiocarbon dating of Dissolved Organic Carbon

Samples from the dark flux incubations from ambient (n=2) and elevated treatments (n=2) at 10.5 d analyzed for $^{14}C$ of DOC. The ambient samples failed to successfully graphitize during analysis and were lost, likely due to low DOC concentrations. Samples were selected from the dark flux to target the high concentration measurements for DOC that occurred during respiration and to avoid the potentially confounding signal from newly produced extracellular polymeric substances from diatoms that is expected during light periods. The $^{14}C$-DOC samples were analyzed by accelerator mass spectrometry at the Australian Nuclear Science and Technology Organisation[37]. DOC samples were acidified to pH < 2 and dried under vacuum in a rotary evaporator. The residue was heated in a glass tube containing CuO, Ag, and Cu wire to 600˚C for 2 h to remove any sulfur compounds. The sample was then graphitized by reduction with hydrogen gas in the presence of an iron catalyst at 600˚C. Results were reported in percent Modern carbon (pMC) normalized against the $\delta^{13}C$ of the graphite, with an average 1σ error of the AMS readings at ± 0.3 pMC. Radiocarbon age calculations are presented as 'conventional radiocarbon ages' (years Before Present)[38] and not calendar ages using the equation:

$$^{14}C\ age = -8033 \times \ln[(1+ \Delta^{14}C_{initial} / 1000) / (1+ \Delta^{14}C_{atm} / 1000)]\ ^{14}C\ years$$

with $\Delta^{14}C_{initial}$ as the initial radiocarbon content and $\Delta^{14}C_{atm}$ as the radiocarbon content of the atmosphere at the time of deposition.

## Results and Discussion

### Treatment application and labeled exports

The pulse of labeled MPB-C produced by the *in situ* MPB community (1549 µmol $^{13}C$ $m^{-2}$ added as OC) quickly underwent processing by the microbial community. Significantly more of this newly fixed C was remineralized and exported as $DI^{13}C$ under increased nutrient availability than under ambient conditions (two-way ANOVA: treatment $F_{1,19}$=12.3, $p$<0.01, day $F_{4,19}$ =2.4, $p$=0.1, interaction $p$=0.08; Fig. 3A). Increased export in the elevated treatment was observed at 0.5 d after nutrient addition and maintained for at least 10.5 d. Cumulative export of $DO^{13}C$ was similar across treatments, with lower $DO^{13}C$ fluxes than $DI^{13}C$ fluxes, and increased significantly over 10.5 d (two- way ANOVA: treatment $F_{1,19}$=4.3, $p$=0.02, day $F_{4,19}$ =9.4, $p$<0.01, interaction $p$=0.9; Fig.3B).

### Increased DOC Efflux

MPB-C stimulated breakdown and export of pre-existing sediment OM and increased the efflux of DOC derived from this material to the water column under increased nutrient concentrations (Elevated treatment, 10.5 d, Fig. 4B). Increased efflux of DOC from pre-existing sediment OM in the elevated treatment was significantly in excess of the ambient treatment across 10.5 d (two-way ANOVA: treatment $F_{1,19}$=51.2; $p$<0.001, day $F_{4,19}$=27.6, $p$<0.001; interaction $p$<0.001). Efflux of DOC derived from sediment OM was larger for the elevated treatment (1.2-6.6 ×; Fig. 4B) than for the only positive efflux observed within the ambient treatment (10.5 d; 670 ± 212 µmol C $m^{-2}$ $h^{-1}$; Fig. 4B). Because we were able to partition

completely both the non-labeled and labeled pools of C that composed DIC and DOC effluxes, we were able to identify a substantial increase in the efflux of unlabeled DOC, which comprised >99% of the cumulative total C export (Elevated 10.5 d, Fig. 4B) under increased nutrient availability. The statistically significant differences in fluxes between treatments indicate that the effects observed were robust to low power caused by limited replication (n=2 per time period).

Global DOC fluxes from intertidal zones are estimated at 7 to 10 Tg C $yr^{-1}$(minimum to maximum) [33] with similarly scaled estimates from the elevated treatment in this study resulting in estimated DOC fluxes of 46.9 to 67.0 Tg C $yr^{-1}$. Although this estimate reflects a 6.7 × increase in DOC flux measured for this site-specific study and has considerable associated error, the magnitude of increased export of DOC from the elevated treatment is concerning given that the global estimate for total OC burial within coastal sediments is at a similar scale (300 Tg C $yr^{-1}$) [3]. Our estimate of enhanced DOC flux likely overemphasizes the global role of priming effects, given that not all intertidal zones are microphytobenthos-dominated. However, our estimate would conservatively decrease current organic carbon burial estimates by ~8 to 11% using an estimated spatial occurrence of 50%. The scale of this effect highlights that the DOC flux increase stimulated by priming effects are potentially globally significant for enhancing the removal of refractory carbon from coastal sediments. The global estimate provided has been calculated from fluxes measured from a single site and is inherently uncertain. The estimate does not incorporate spatial and temporal variation and/or the impact of ex situ incubation on sediment processing. . This estimate was derived from a nutrient amended treatment during a short-term period and is predominantly intended to highlight the potential for priming to contribute significantly to the global organic matter budget.

Characterization of exported DOC

To verify that effluxed material resulted from the additional breakdown of old and refractory sediment OM, we used three approaches: UV-visible absorption spectra (Fig. 5A & B), C:N (Fig. 5C), and $\Delta^{14}C$ dating. We characterized the DOC efflux for both treatments by UV-visible absorption spectra, using both slope ratio ($S_R$)[35] and SUVA 254[36] to characterize size and relative aromaticity of the molecules comprising the effluxed DOC. Molecules comprising the DOC efflux within the elevated treatment had higher C/N ratios (Fig. 5C), a reduced molecular size (Fig. 5A), increased aromaticity (Fig. 5B), and an inverse relationship between the two treatments across time (Fig. 5A&B). These characteristics all indicate that the DOC produced over 10.5 d in the elevated treatment became more refractory than ambient DOC effluxes. Although increased DOC effluxes can be associated with hypoxic or anoxic events in the sediment[39], the increased export of more refractory molecules in the elevated treatment here occurred under oxic conditions (lowest $O_2$ measurement 4.85 mg $L^{-1}$ at the end of dark period at 10.5 d) with DOC effluxes that were comparable during dark and light periods. It is therefore unlikely that increased DOC efflux was due to either the development of hypoxic or anoxic conditions, or large shifts in redox conditions in the 20 cm sediment cores.

The old radiocarbon age (6855 ± 120 years BP) for DOC in the elevated treatment further showed that old sediment OM was broken down and exported as DOC as a result of priming. The old age of DOC resulting from the breakdown of sediment OM at the study site suggests that the material forming the sediment was composed of older scour material deposited on the mudflat. Flooding within the Richmond River occurs at regular intervals[40,41] and dating of basal core organic matter just upstream from our study site showed an age of 5,312 - 5,583 y BP[42], which is similar to the age of the effluxed DOC. Given the tendency for material composed of older $\Delta^{14}C$ to be less photo-reactive and bioavailable, and the refractory nature of the characterized

compounds, the exported material is likely directly transported to the coastal shelf with minimal reworking after hydrolysis by heterotrophic bacteria in the sediment.

Is this priming?

The higher C:N ratio, smaller molecular size, and radiocarbon age of effluxed DOC in the elevated treatment provide compelling evidence that priming occurred within the intertidal sediments in this study. Microbial processing of MPB-C under elevated nutrient loads resulted in carbon released from breakdown of older sediment OM via hydrolysis[43] that was largely exported via DOC effluxes (Fig.1B). The combination of a labile pulse of C, enhanced by increased nutrient availability, stimulated microbial degradation of older refractory OM, likely through increased bacterial production of hydrolytic extracellular enzymes[44]. Although we did not measure enzyme activity, increased breakdown of sediment OM was indicated by the old radiocarbon age and increased aromaticity of the increased DOC effluxes produced in the elevated treatment (Fig. 5A & B). Unfortunately, no direct comparison can be made for the ambient treatment radiocarbon age, likely due to the low concentration of DOC being insufficient for analysis. The pulse of labile MPB-C was strongly retained within sediment OM in both treatments across 3.5 d (Fig. 3), with relatively low effluxes for $DI^{13}C$ and $DO^{13}C$ across this time resulting in relatively long estimates for MPB-C turnover (419 d ambient vs 199 d elevated)[26]. Strong short-term retention of MPB-C in both treatments indicates that the microbial community readily used the newly produced labile $^{13}C$ and subsequently recycled respired $DI^{13}C$ to support productivity.

Respiration of older sediment OM provided increased DIC to support MPB productivity (Fig. 3A) within a system that has been previously found to be DIC-limited[24]. Algal production

supported by recycled DIC was captured by oxygen fluxes and production to respiration measurements, as increased bacterial respiration of OM increasingly offset initial productivity in the elevated treatment (Supplemental Fig. 1). However, these dynamics are not supported by consideration of DIC fluxes alone, as the considerable primary productivity that occurred during light periods offset the respired carbon that would have been exported in a less productive system. A potential solution to this problem could be to include DOC exports from sediment OM, a byproduct of remineralization that has not previously been considered in evaluation of priming effects (Fig. 3B & 4B). It is important to acknowledge that DOC exports can also consist of MPB exudates, therefore exported DOC must be characterized as having arisen from bacterial remineralization of sediment OM. Characterization of DOC effluxes (using both molecular and radiocarbon techniques) serves to confirm that the DOC is not predominately composed of labile compounds copiously produced by MPB. Inclusion of the fluxes of DIC and DOC together enabled more complete accounting of the export of C that arose during a priming event within a highly productive benthic environment.

## Implications

We posit that some of the difficulty identifying positive priming effects in aquatic systems[11] may be due to the examination of solely heterotrophic relationships during the processing of OM. Exclusion of any interactions with primary producers misses potential co-metabolism or processes that occur in situ (Fig. 1 bottom), including the recapture and recycling of the products of priming ($CO_2$/DIC) during high productivity. This is largely an artefact of priming studies having been developed in soils[5,45] where remineralization is has been considered to be the sole process affecting the respiratory $CO_2$ evolution, primary producers have not been included, and $CO_2$ is easily monitored as a production only function (Fig. 1 top). In aquatic

systems, the evolution of $CO_2$ is likely to be at least partially offset by primary productivity in many settings where priming is likely to occur (e.g. shallow benthic microbial communities, suspended estuarine microbial communities). Therefore $CO_2$ production alone does not adequately represent microbial heterotrophic processing in eupthotic systems. Further development of a standard metric for quantifying potential priming that accounts for both respiration and production would be useful in investigating the dynamics of co-metabolism in communities containing both microbial producers and bacterial heterotrophs.

This study suggests that nutrient enrichment of coastal systems[46] may be an additive factor in stimulating the decomposition and export of C from sediment OM. Increased nutrient availability stimulated increased efflux of DOC sourced from older OM most likely through increased bioavailability of OM to heterotrophic bacteria. Bacterial processing increased export of sediment OC that was previously immobilized and unavailable for processing and export. DIC and nutrients that arose from bacterial remineralization likely supported MPB productivity and were recycled within the sediment by co-metabolism within the microbial community. Increased microbial recycling resulted in increased contribution of uncharacterized material to $^{13}C$ within sediment OM in the elevated treatment[32]. Therefore, inclusion of the byproducts of remineralization from sediment OM (DOC) allows for more complete accounting of the C arising from priming effects, especially in highly productive systems.

Increased remineralization and export of DOC under elevated nutrient conditions provides a potential priming effect resulting in increased C export from estuarine sediments to the continental shelves and should be further considered within blue carbon inventories for coastal sediments. This study has shown that immobilized OM in shallow photic sediments that is otherwise considered to be non-reactive and buried may become bioavailable through the

391 combination of benthic algal production and elevated nutrient inputs. Inclusion of the DOC
392 export from sediment OM in priming studies may allow identification of priming effects in
393 systems that include primary producers. Further development of this method has considerable
394 potential for broad application to aquatic systems containing algal producers.

395 **References**


396 1 Glud, R. N. Oxygen dynamics of marine sediments. *Marine Biology Research* **4**, 243-289,
397 doi:10.1080/17451000801888726 (2008).
398 2 Raymond, P. A. & Bauer, J. E. Use of $^{14}C$ and $^{13}C$ natural abundances for evaluating riverine,
399 estuarine, and coastal DOC and POC sources and cycling: a review and synthesis. *Organic*
400 *Geochemistry* **32**, 469-485, doi:http://dx.doi.org/10.1016/S0146-6380(00)00190-X (2001).
401 3 Bauer, J. E., Cai, W..-J., Raymond, P.A., Bianchi, T.S., Hopkinson, C.S., Regnier, P.A.G. The changing carbon
402 cycle of the coastal ocean. *Nature* **504**, 61-70, doi:10.1038/nature12857 (2013).
403 4 Cai, W.-J. Estuarine and Coastal Ocean Carbon Paradox: CO2 Sinks or Sites of Terrestrial Carbon
404 Incineration? *Annual Review of Marine Science* **3**, 123-145, doi:doi:10.1146/annurev-marine-
405 120709-142723 (2011).
406 5 Kuzyakov, Y., Friedel, J. & Stahr, K. Review of mechanisms and quantification of priming effects.
407 *Soil Biology and Biochemistry* **32**, 1485-1498 (2000).
408 6 Blagodatskaya, E. & Kuzyakov, Y. Mechanisms of real and apparent priming effects and their
409 dependence on soil microbial biomass and community structure: critical review. *Biology and*
410 *Fertility of Soils* **45**, 115-131, doi:10.1007/s00374-008-0334-y (2008).
411 7 Bianchi, T. S. The role of terrestrially derived organic carbon in the coastal ocean: A changing
412 paradigm and the priming effect. *Proceedings of the National Academy of Sciences* **108**, 19473-
413 19481, doi:10.1073/pnas.1017982108 (2011).
414 8 Hee, C. A., Pease, T. K., Alperin, M. J. & Martens, C. S. Dissolved organic carbon production and
415 consumption in anoxic marine sediments: A pulsed-tracer experiment. *Limnology and*
416 *oceanography* **46**, 1908-1920 (2001).
417 9 van Nugteren, P. Moodley, L., Brummer, G.-J., Heip, C.H.R., Herman, P.M.J., and Middelburg, J.J. Seafloor
418 ecosystem functioning: the importance of organic matter priming. *Marine Biology* **156**, 2277-
419 2287, doi:10.1007/s00227-009-1255-5 (2009).
420 10 Bianchi, T. S., Thornton, D.C.O., Yvon-Lewis, S.A., King, G.M., Eglinton, T.I., Shields, M.R., Ward, N.D., Curtis, J.
421 Positive priming of terrestrially derived dissolved organic matter in a freshwater microcosm
422 system. *Geophysical Research Letters* **42**, 5460-5467, doi:10.1002/2015GL064765 (2015).
423 11 Bengtsson, M. M., Attermeyer, K. & Catalán, N. Interactive effects on organic matter processing
424 from soils to the ocean: are priming effects relevant in aquatic ecosystems? *Hydrobiologia*,
425 doi:10.1007/s10750-018-3672-2 (2018).
426 12 Hannides, A. K. & Aller, R. C. Priming effect of benthic gastropod mucus on sedimentary organic
427 matter remineralization. *Limnology and Oceanography* **61**, 1640-1650 (2016).
428 13 Gontikaki, E., Thornton, B., Cornulier, T. & Witte, U. Occurrence of priming in the degradation of
429 lignocellulose in marine sediments. *PLoS ONE* **10**, doi:10.1371/journal.pone.0143917 (2015).

14 Koch, B. P., Kattner, G., Witt, M. & Passow, U. Molecular insights into the microbial formation of marine dissolved organic matter: Recalcitrant or labile? *Biogeosciences* **11**, 4173-4190, doi:10.5194/bg-11-4173-2014 (2014).

15 Catalán, N., Kellerman, A. M., Peter, H., Carmona, F. & Tranvik, L. J. Absence of a priming effect on dissolved organic carbon degradation in lake water. *Limnology and Oceanography* **60**, 159-168, doi:10.1002/lno.10016 (2015).

16 Bengtsson, M.M., Wagner, K., Burns, N.R., Herberg, E.R., Wanek, W., Kaplan, L.A., Battin, T. J. No evidence of aquatic priming effects in hyporheic zone microcosms. *Scientific Reports* **4**, 5187 (2014).

17 Danger, M., Cornut, J., Chauvet, E., Chavez, P., Elger, A., Lecerf, A., Benthic algae stimulate leaf litter decomposition in detritus-based headwater streams: a case of aquatic priming. *Ecology* **94**, 1604-1613 (2013).

18 Guenet, B. Danger, M., Harrault, L., Allard, B., Jauset-Alcala, M., Bardoux, G., Benest, D., Abbadie, L. Lacroix, G. Fast mineralization of land-born C in inland waters: First experimental evidences of aquatic priming effect. *Hydrobiologia* **721**, 35-44, doi:10.1007/s10750-013-1635-1 (2014).

19 Oakes, J. M., Eyre, B., D., Middelburg, J. J. & Boschker, H. T. S. Composition, production, and loss of carbohydrates in subtropical shallow subtidal sandy sediments: Rapid processing and long-term retention revealed by $^{13}$C-labeling. *Limnology and Oceanography* **55**, 2126-2138 (2010).

20 Kristensen, E. & Holmer, M. Decomposition of plant materials in marine sediment exposed to different electron acceptors (O 2, NO 3−, and SO 4 2−), with emphasis on substrate origin, degradation kinetics, and the role of bioturbation. *Geochimica et Cosmochimica Acta* **65**, 419-433 (2001).

21 Guenet, B., Danger, M., Abbadie, L. & Lacroix, G. Priming effect: bridging the gap between terrestrial and aquatic ecology. *Ecology* **91**, 2850-2861 (2010).

22 Heimann, M. & Reichstein, M. Terrestrial ecosystem carbon dynamics and climate feedbacks. *Nature* **451**, 289-292 (2008).

23 ANZECC. *Australia and New Zealand guidelines for fresh and marine water quailty*, <https://www.waterquality.gov.au/guidelines/anz-fresh-marine> (2018).

24 Oakes, J. M. & Eyre, B. D. Transformation and fate of microphytobenthos carbon in subtropical, intertidal sediments: Potential for long-term carbon retention revealed by 13C-labeling. *Biogeosciences* **11**, 1927-1940 (2014).

25 Riekenberg, P. M., Oakes, J. M. & Eyre, B. D. Uptake of dissolved organic and inorganic nitrogen in microalgae-dominated sediment: comparing dark and light *in situ* and *ex situ* additions of $^{15}$N. *Marine Ecology Progress Series* **571**, 29-42 (2017).

26 Riekenberg, P. M., Oakes, J. M. & Eyre, B. D. Short-term fate of intertidal microphytobenthos carbon under enhanced nutrient availability: a $^{13}$C pulse-chase experiment. *Biogeosciences* **15**, 2873-2889 (2018).

27 Cloern, J. E., Abreu, P.C., Carstensen, J., Chauvaud, L., Elmgren, R., Grall, J., Greening, H., Johansson, J. O. R., Kahru, M., Sherwood, E.T., Xu, J., Yin, K. Human activities and climate variability drive fast-paced change across the world's estuarine–coastal ecosystems. *Global Change Biology* **22**, 513-529, doi:10.1111/gcb.13059 (2016).

28 Eyre, B. D. Regional evaluation of nutrient transformation and phytoplankton growth in nine river-dominated sub-tropical east Australian estuaries. *Marine Ecology Progress Series* **205**, 61-83, doi:10.3354/meps205061 (2000).

29 Ferguson, A. J. P., Eyre, B. D. & Gay, J. M. Benthic nutrient fluxes in euphotic sediments along shallow sub-tropical estuaries, northern New South Wales, Australia. *Aquatic Microbial Ecology* **37**, 219-235, doi:10.3354/ame037219 (2004).

30 Eyre, B. D., Maher, D. T. & Squire, P. Quantity and quality of organic matter (detritus) drives N2 effluxes (net denitrification) across seasons, benthic habitats, and estuaries. *Global Biogeochemical Cycles* **27**, 1083-1095, doi:10.1002/2013GB004631 (2013).
31 Elvridge, C. D., Keith, D. M., Tuttle, B. T. & Baugh, K. E. Spectral identification of lighting type and character. *Sensors* **10**, 3961-3988, doi:10.3390/s100403961 (2010).
32 Oakes, J. M., Eyre, B. D., Ross, D. J. & Turner, S. D. Stable Isotopes Trace Estuarine Transformations of Carbon and Nitrogen from Primary- and Secondary-Treated Paper and Pulp Mill Effluent. *Environmental Science & Technology* **44**, 7411-7417, doi:10.1021/es101789v (2010).
33 Maher, D. T. & Eyre, B. D. Benthic fluxes of dissolved organic carbon in three temperate Australian estuaries: Implications for global estimates of benthic DOC fluxes. *Journal of Geophysical Research: Biogeosciences* **115**, doi:10.1029/2010JG001433 (2010).
34 Jickells, T. & Rae, J. Biogeochemistry of Intertidal Sediments. *Biogeochemistry of Intertidal Sediments, Edited by TD Jickells and JE Rae, pp. 205. ISBN 0521483069. Cambridge, UK: Cambridge University Press, June 1997.*, 205 (1997).
35 Helms, J. R. Stubbins, A., Ritchie, J.D., Minor, E.C., Kieber, D.J., Mopper, K. Absorption spectral slopes and slope ratios as indicators of molecular weight, source, and photobleaching of chromophoric dissolved organic matter. *Limnology and Oceanography* **53**, 955-969 (2008).
36 Weishaar, J. L., Aiken, G.R., Bergamaschi, B.A., Fram, M.S., Fujii, R., Mopper, K. Evaluation of specific ultraviolet absorbance as an indicator of the chemical composition and reactivity of dissolved organic carbon. *Environmental Science and Technology* **37**, 4702-4708 (2003).
37 Fink, D., Hotchkis, M., Hua, Q., Jacobsen, G., Smith, A. M., Zoppi, U., Child, D., Mifsud, C., van der Gaast, H., Williams, A., Williams, M. The ANTARES AMS facility at ANSTO. *Nuclear Instruments and Methods in Physics Research Section B: Beam Interactions with Materials and Atoms* **223–224**, 109-115, doi:http://dx.doi.org/10.1016/j.nimb.2004.04.025 (2004).
38 Stuiver, M. & Polach, H. A. Reporting of $^{14}C$ data. *Radiocarbon* **19**, 355-363 (1977).
39 Skoog, A. C. & Arias-Esquivel, V. A. The effect of induced anoxia and reoxygenation on benthic fluxes of organic carbon, phosphate, iron, and manganese. *Science of the total environment* **407**, 6085-6092 (2009).
40 Eyre, B. Water quality changes in an episodically flushed sub-tropical Australian estuary: A 50 year perspective. *Marine Chemistry* **59**, 177-187, doi:http://dx.doi.org/10.1016/S0304-4203(97)00070-4 (1997).
41 McKee, L. J., Eyre, B. D. & Hossain, S. Transport and retention of nitrogen and phosphorus in the sub-tropical Richmond River estuary, Australia – A budget approach. *Biogeochemistry* **50**, 241-278, doi:10.1023/a:1006339910533 (2000).
42 Logan, B., Taffs, K., Eyre, B. & Zawadski, A. Assessing changes in nutrient status in the Richmond River estuary, Australia, using paleolimnological methods. *J Paleolimnol* **46**, 597-611, doi:10.1007/s10933-010-9457-x (2011).
43 Arnosti, C. Microbial Extracellular Enzymes and the Marine Carbon Cycle. *Annual Review of Marine Science* **3**, 401-425, doi:doi:10.1146/annurev-marine-120709-142731 (2011).
44 Steen, A. D., Quigley, L. N. M. & Buchan, A. Evidence for the Priming Effect in a Planktonic Estuarine Microbial Community. *Frontiers in Marine Science* **3**, doi:10.3389/fmars.2016.00006 (2016).
45 Kuzyakov, Y. Priming effects: Interactions between living and dead organic matter. *Soil Biology and Biochemistry* **42**, 1363-1371 (2010).
46 Cloern, J. E. Our evolving conceptual model of the coastal eutrophication problem. *Marine ecology progress series* **210**, 223-253 (2001).

Acknowledgements: We thank I. Alexander, M. Carvalho, N. Carlson-Perret, R. Murray, B. Riekenberg, and J. Riekenberg for technical assistance and field support. Funding: This work was supported by grants from the Australian Research Council (ARC), specifically an Early Career Research Award to J.M.O (DE120101290) and a Discovery Project to B.D.E. (DP160100248). Author contributions: P.M.R., J.M.O., and B.D.E. conceived the project and designed the experiment, P.M.R. and J.M.O. performed the experiment processed samples, P.M.R., J.M.O. and B.D.E. analyzed the data, and P.M.R. wrote the manuscript with input from J.M.O. and B.D.E. Competing Interests: The authors declare that they have no competing interests. Data and materials availability: All data needed for evaluation of the conclusions within this paper are present in the paper and/or Supplementary Materials, but additional data is available from authors upon request.

Supplementary Materials:

Table S1: $\delta^{13}C$ (‰) values for DIC and DOC diel fluxes across the 10.5 d incubation period.

S1: Oxygen fluxes and production/respiration measurements.

## Figures

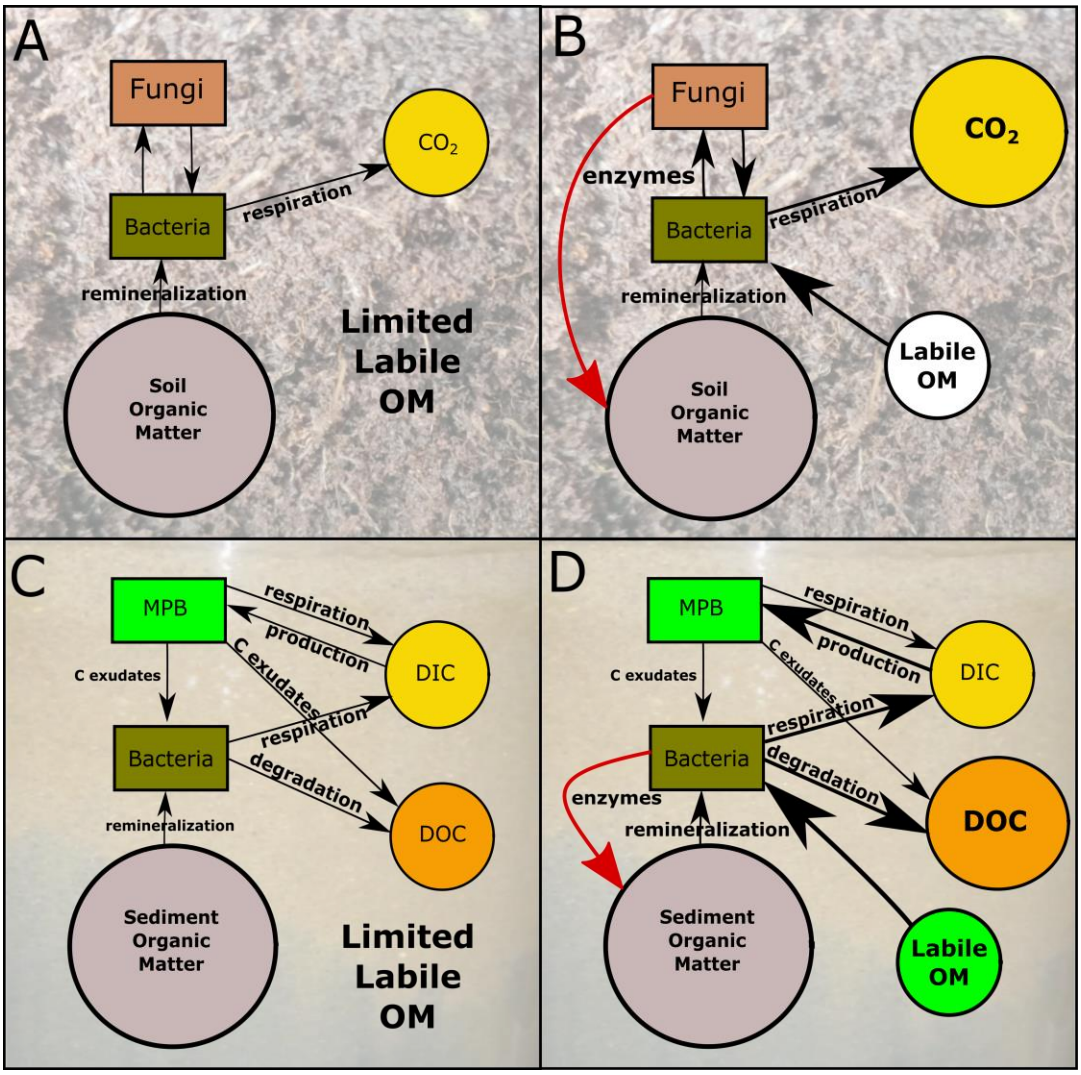


**Figure 1:** Fluxes of C within heterotophic dominated soil (top) and autotrophic dominated benthic sediment (bottom) under normal (left panels A and C) and B) and priming (right panels, B and D) scenarios. The red arrows indicate stimulated production of hydrolytic enzymes by fungi (B) and heterotrophic bacteria (D). Note the bi-directional flows of carbon associated with productive benthic sediments. Soil conceptual diagram (top) adapted from Kuzyakov (2010) (30). Photo credit: Philip Riekenberg, NIOZ.

547

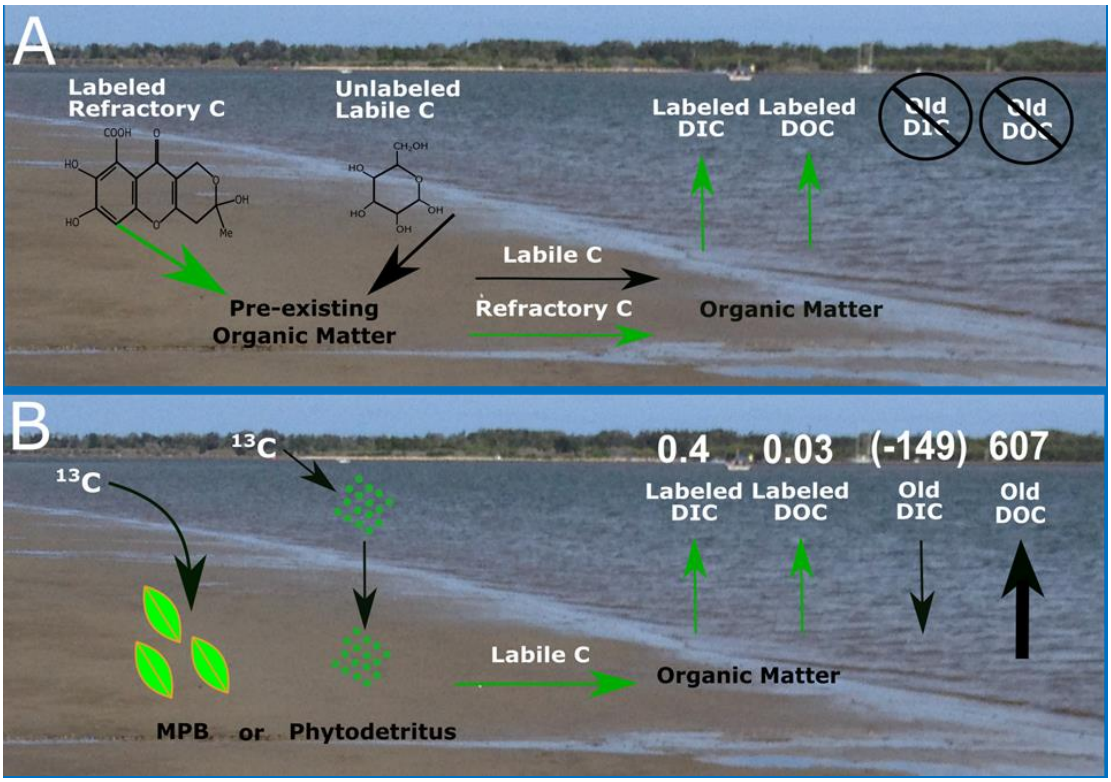


548

549 **Figure 2:** Method diagram comparing priming addition methods. A) Priming experiments
550 typically introduce $^{13}C$-labeled labile and/or refractory material to sediment OM. The export of
551 labeled material can then be traced as additional export occurs, but the unlabeled OM pool is
552 muddled, making it impossible to track decomposition of pre-existing sediment OM. B)
553 Additions of $^{13}C$-labeled algal-derived carbon from prepared phytodetritus or label additions
554 processed by the *in situ* microphytobenthos community allow for simultaneous quantification of
555 both non-labeled and labeled DIC and DOC effluxes. In the current study the combined addition
556 of microphytobenthos (MPB) derived C and nutrients enhanced export of both pre-existing C
557 from sediment OM, primarily as DOC, as well as labeled DIC. Numbers indicate cumulative C
558 fluxes observed for the elevated treatment in mmol C $m^{-2}$ across 10.5 d. Photo credit: Philip
559 Riekenberg, NIOZ.

560

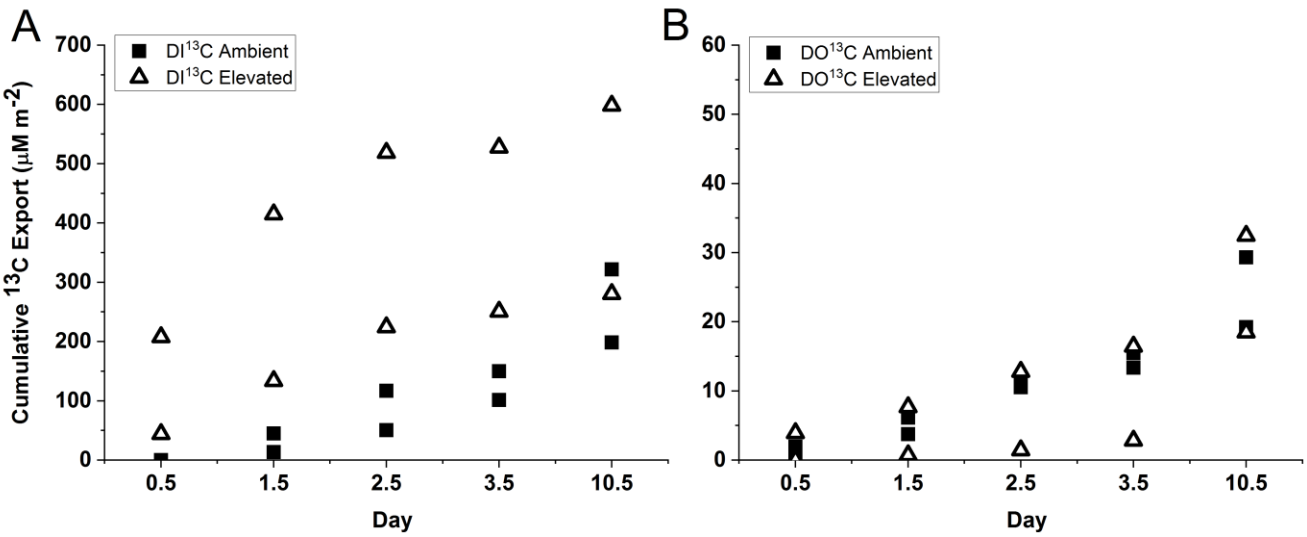


5

562 **Figure 3:** Cumulative export of A) $DI^{13}C$ and B) $DO^{13}C$ from the sediment for individual
563 replicates within each of the ambient and elevated treatment applications. Export of $^{13}C$
564 represents microbial utilization and export of fixed microphytobenthos carbon from the treatment
565 application. $DI^{13}C$ export was significantly higher in the elevated treatment than ambient (two-
566 way ANOVA: treatment $F_{1,19}=12.3$, $p<0.01$, day $F_{4,19}=2.4$, $p=0.1$, interaction $p=0.08$). Further
567 indication of core replicates within each treatment is provided as Supplemental Figure 2.

568

569

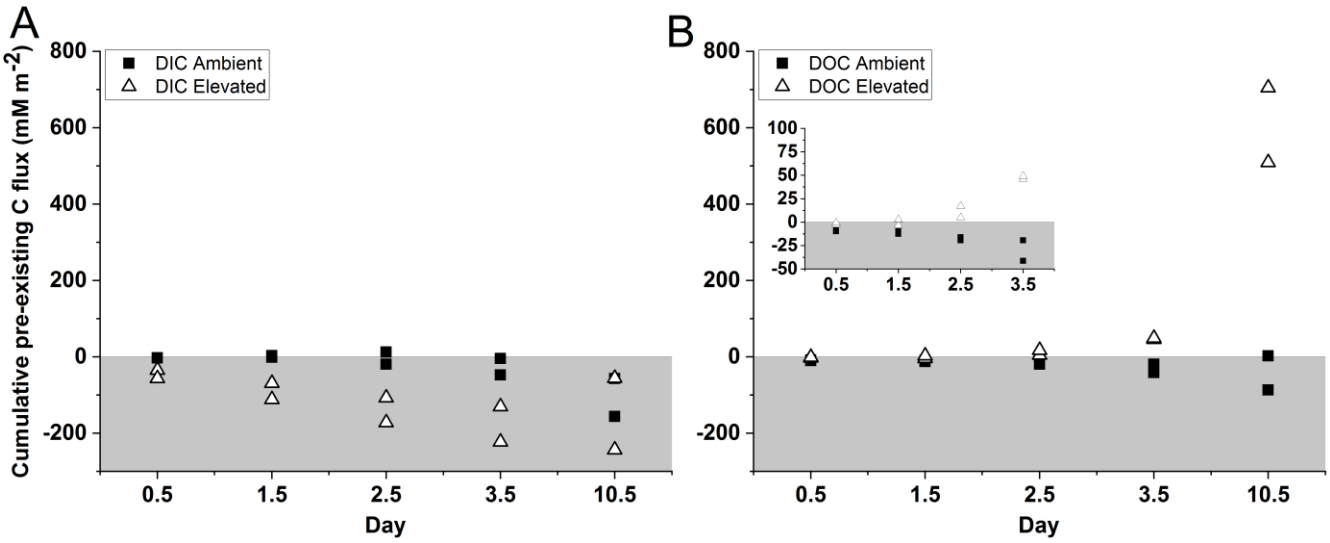


**Figure 4:** Cumulative flux of non-labeled A) DIC and B) DOC. DOC flux was significantly higher in the elevated treatment than ambient (two-way ANOVA: treatment $F_{1,19}$=51.2; $p$<0.001, day $F_{4,19}$=27.6, $p$<0.001; interaction $p$<0.001) and represents export derived from pre-existing sediment OM. Inset graph highlights the differences between ambient and elevated fluxes of DOC at 0.5-3.5 d. Grey region indicates uptake of carbon.

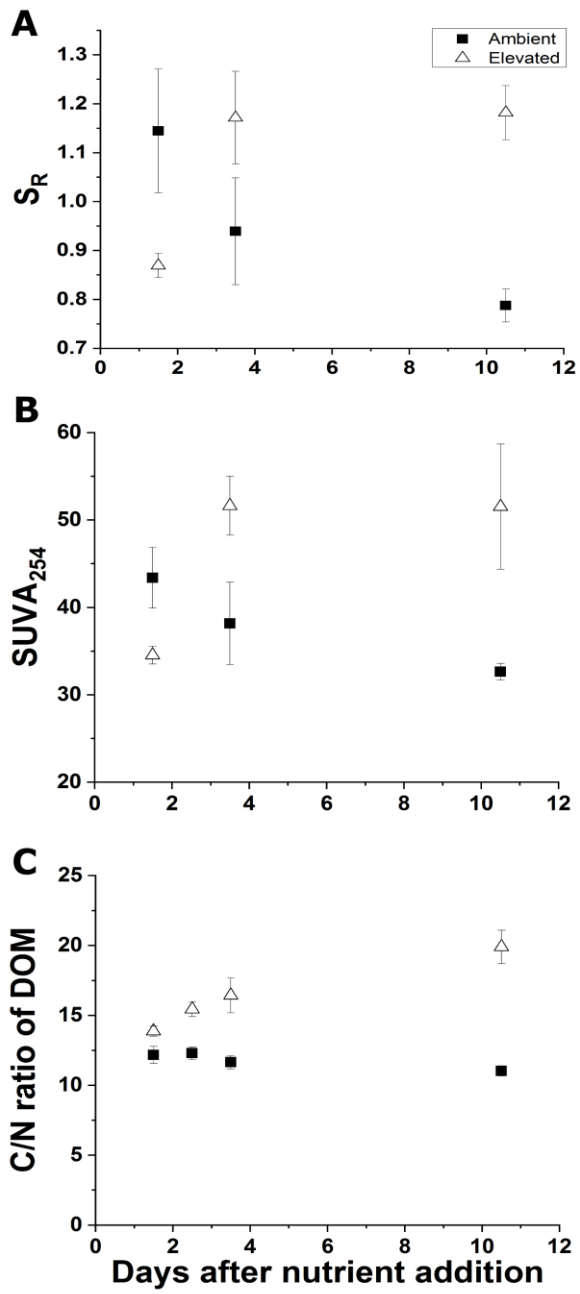


**Figure 5:** Characterization of DOC efflux via A) slope ratio of DOC for both treatments, B) $SUVA_{254}$ of DOC for both treatments, and C) Molar C/N ratios for dissolved organic material efflux. All measurements for indicated treatments were performed on duplicate cores (mean±SD).